

CALCULATION OF CSR IMPEDANCE USING MESH METHOD

D. Zhou*, KEK, 1-1 Oho, Tsukuba, Ibaraki 305-0801, Japan

Abstract

A new code CSRZ was developed to investigate the longitudinal coherent synchrotron radiation (CSR) impedance for a single or a series of bending magnets. To calculate CSR impedance, the mesh method developed by T. Agoh and K. Yokoya [1] was adapted to the case of a curved rectangular chamber with variable bending radius. The method is based on the integration of the parabolic equation in the frequency domain in a curvilinear coordinate system. In the code CSRZ, the curvature of the beam trajectory can be set to be an arbitrary function of the distance along the beam orbit. Thus it allows calculating CSR impedance generated by either a single bending magnet or a series of bending magnets. In this paper, we first describe the code and formalism for CSR calculation. Then we apply the code to calculate the longitudinal CSR impedance using an example appearing in the compact energy recovery linac (cERL) project at KEK.

INTRODUCTION

The mesh method was devised by Agoh and Yokoya and has been used to calculate the longitudinal CSR impedance in a single bending magnet [1]. The most important idea was based on paraxial approximation of Maxwell's equations. A simplified set of parabolic equations was found to describe the evolutions of CSR fields, i.e.

$$\frac{\partial \vec{E}_\perp}{\partial s} = \frac{i}{2k} \left[\nabla_\perp^2 \vec{E}_\perp - \frac{1}{\epsilon_0} \nabla_\perp \rho_0 + 2k^2 \left(\frac{x}{R(s)} - \frac{1}{2\gamma^2} \right) \vec{E}_\perp \right], \quad (1)$$

where \vec{E}_\perp is the transverse electric field, and $R(s)$ is the bending radius at distance s along the beam orbit. ϵ_0 is the vacuum permittivity. γ is the Lorentz factor, representing the beam energy. The term of $1/\gamma^2$ indicates the normal space-charge effect. The beam is assumed to be rigid, i.e. the beam charge density ρ_0 does not vary along s . Equation (1) also describes the field evolution in a straight chamber where the inverse bending radius is zero. With paraxial approximation, the longitudinal electric field is approximated by

$$E_s = \frac{i}{k} \left(\nabla_\perp \cdot \vec{E}_\perp - \mu_0 c J_s \right), \quad (2)$$

where μ_0 is the vacuum permeability, c is the speed of light in vacuum, and $J_s = \rho_0 c$ is the current density.

The spatially discretized version of Eq. (1) was solved by an iterative procedure on a uniform grid. It was pointed out in Ref. [1] that this mesh method is very flexible and can be extended in a number of ways.

The original motivation of developing an independent code, i.e. CSRZ, was intended to study the multi-bend CSR interference in a storage ring. In CSRZ, the beam is assumed to have a point charge form in the longitudinal direction. Then the longitudinal CSR impedance is calculated by directly integrating E_s over s

$$Z_\parallel(k) = -\frac{1}{q} \int_0^\infty E_s(x_c, y_c) ds \quad (3)$$

where (x_c, y_c) denotes the center of the beam in the transverse x - y plane. The appearance of the minus sign in Eq. (3) is due to the convention of the beam instability formalism.

The code CSRZ has been used to investigate the multi-mode interference in a long bending magnet with toroidal pipe [2], the multi-bend interference in a series of bending magnets [3], the coherent undulator radiation impedance [4], and the CSR field profiles inside a vacuum chamber [5]. In this paper, the main features of CSRZ are presented first. Then CSR impedance in a single magnet of cERL return loop [6] is calculated. The numerical results are compared with the analytical models.

MAIN FEATURES OF CSRZ

The code CSRZ inherits main features of Agoh's method as described in Ref. [7]. As shown in Eq. (1), the beam trajectory defined by $R(s)$ is assumed to be an arbitrary functions of s . This assumption indicates the most significant feature of CSRZ. The beam trajectory can be generated by a single bending magnet, by a series of bending magnets, or by an undulator or a wiggler. Consequently, the vacuum chamber having a uniform rectangular cross-section adopts the same curvature of the beam trajectory. Freeing $R(s)$ allows CSRZ to investigate the CSR interference between consecutive bending magnets, even coherent wiggler or undulator radiation.

The total field is separated into two parts: the beam self-field in free space and the radiation field inside the vacuum chamber. For an ultra-relativistic beam, the beam field is transverse to the beam orbit and its analytic solution for a bi-Gaussian distribution is known and is independent of s . The boundary conditions should also be modified due to this field separation. The resistive-wall effects has also been taken into account by applying Leontovich boundary condition at the metal chamber surface.

* dmzhou@post.kek.jp

The fields before the beam enters the curved chamber are given by the steady-state Coulomb field of the relativistic beam established in the straight chamber. By solving Poisson's equation of electric potential, the initial conditions are determined. Consequently, the entrance transient effect of CSR is naturally included.

Regarding to the discretization of the field evolution equation, finite-difference scheme is adopted. To avoid numerical oscillations as well as numerical damping, the fields are sampled on a staggered grid with ghost points outside the chamber wall surface introduced to enforce the boundary conditions. The transient effect at the final exit of the curved chamber is treated by connecting an infinite long straight chamber. The CSR fields entering this straight section are decomposed into the sum of simple eigenmodes in a uniform rectangular waveguide. Then the total wake potential is obtained by integrating these modes semi-analytically [8].

The capability of CSRZ is mainly limited by the mesh sizes in the $x - y$ plane and step size in the s direction. With explicit discretization scheme, the mesh and step sizes should be proportional to $k^{-2/3}$ and $k^{-1/3}$ respectively, due to necessary numerical stability conditions [1]. To obtain CSR impedance at extremely high frequency, the computations become unacceptably expensive. The next limitation factors are bending radius and chamber cross-section. Smaller bending radius and larger chamber cross-section lead to longer computing time and more computer memory.

APPLICATION TO COMPACT-ERL AT KEK

The cERL is a test facility under construction at KEK for demonstrating key technologies of GeV-class ERLs. The beam energy with one acceleration is 35 MeV in the first commissioning and will be 125 MeV finally [6]. The rms bunch length is 1-3 ps for normal operation and 0.1 ps or less for bunch compression mode. The bunch charge is 7.7 to 77 pC for normal operation and 77pC or more for bunch compression. The vacuum chamber of the cERL loop basically has a round shape with diameter of 50 mm.

The CSR impedance for a single bend is calculated at different beam energy, as depicted in Fig. 1. The vacuum chamber cross-section is approximated by a square with full size of 50 mm. The bending radius and bending angle for one bend are 1 m and $\pi/4$, respectively. The beam is assumed to locate at the center of the chamber, with transverse beam sizes of $\sigma_x = 0.2$ mm and $\sigma_y = 0.1$ mm. The numerical results are compared with steady-state models in free space [9] and with parallel-plates shielding [1]. From the figures, both numerical and analytical results show that at frequencies lower than $k_{th} = \pi\sqrt{R/b^3}$ [10], the CSR waves are strongly shielded, mainly due to the existence of the upper and lower chamber walls. The outer-wall of the chamber reflects the trailing radiation fields back to the beam and causes fluctuations

in the impedance. The inner-wall of the chamber shields the overtaking fields and changes the slope of the imaginary part of the impedance [2]. The imaginary impedances show remarkable difference in the slope at beam energies of $E = 35$ MeV and $E = 125$ MeV. This difference is due to the normal space-charge effect related to the $1/\gamma^2$ term. It suggests that normal space-charge effects can be comparable to CSR effects at the beam energy of 35 MeV. At beam energy of 125 MeV or higher, normal space-charge effects are fairly negligible.

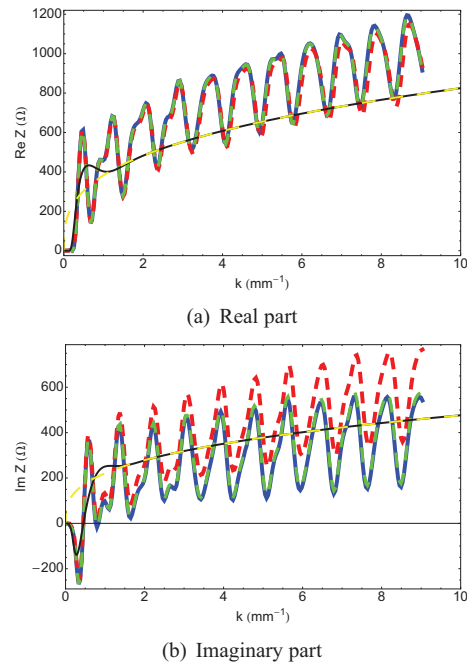


Figure 1: CSR impedance for a single bend in the cERL return loop. The CSR in the drift chamber after the exit of the bend is taken into account. Blue solid lines: $\gamma = \infty$; red dashed lines: $\gamma = 68.5$ ($E = 35$ MeV); green dashed lines: $\gamma = 244.6$ ($E = 125$ MeV); black solid lines: steady-state parallel plates model; yellow dashed lines: steady-state free space model.

The longitudinal wake potential, indicating energy kick along a beam bunch, can be calculated from impedance with specified bunch profile. As shown in Fig. 2, first we assume Gaussian bunch lengths of $\sigma_t = 1, 2, 3$ ps and calculate the CSR wake potentials from the impedances shown in Fig. 1. Because we only considered the normal space-charge effect in a chamber length of $L_b = 0.7854$ m, the space-charge effect is almost invisible from the wake potentials. If we take into account the space-charge fields distributed around the whole loop, space-charge effect can become remarkable at short bunch length of $\sigma_t = 1$ ps in the low beam energy of 35 MeV.

In Fig. 3, we compare the CSRZ results with the 1D model adopted in ELEGANT code [11, 12]. At this point, the drift CSR, which will be checked in next paragraphs, is ignored tentatively. One observes that in general CSRZ agrees with the 1D model from Saldin *et al.* in predic-

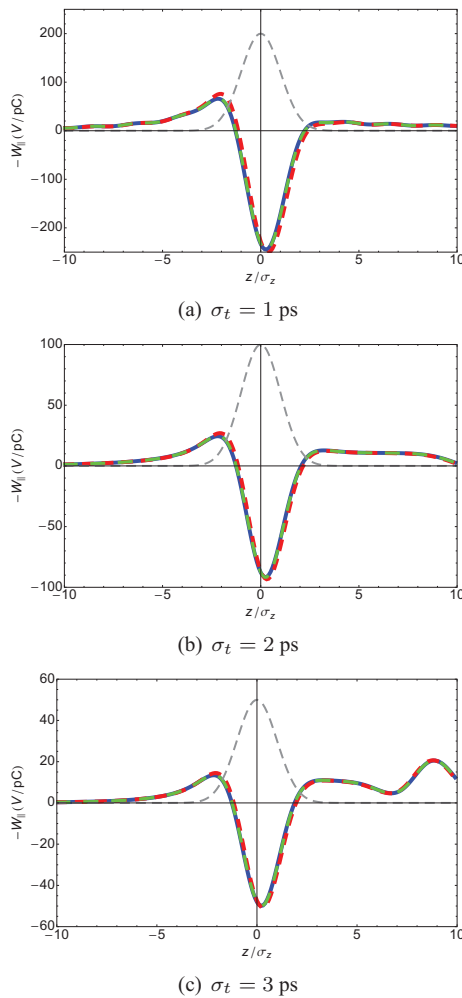


Figure 2: CSR wake potentials for a single bend in the cERL return loop with Gaussian bunch lengths of $\sigma_t = 1, 2, 3$ ps. The drift CSR is taken into account. Blue solid lines: $\gamma=\infty$; red dashed lines: $\gamma=68.5$ ($E=35$ MeV); green dashed lines: $\gamma=244.6$ ($E=125$ MeV); gray dashed lines: Gaussian bunch profile.

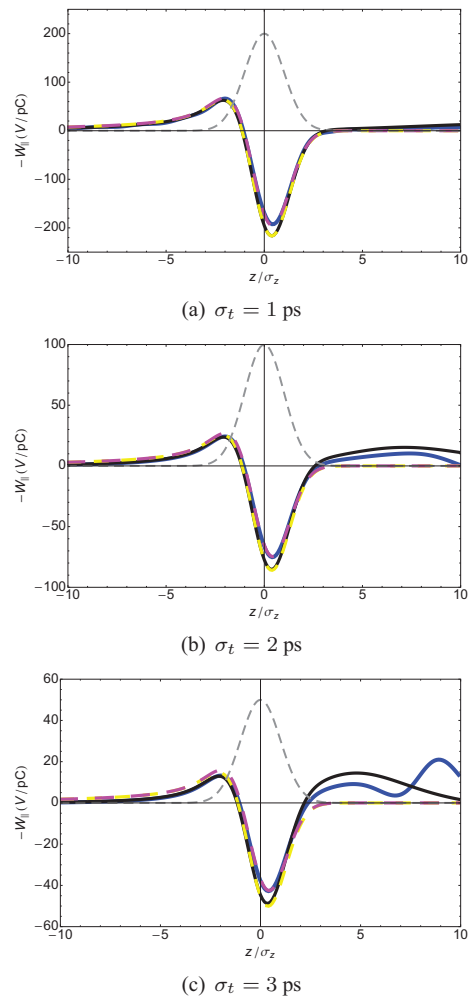


Figure 3: CSR wake potentials for a single bend in the cERL return loop with Gaussian bunch lengths of $\sigma_t = 1, 2, 3$ ps and $\gamma = \infty$. The drift CSR is not taken into account. Blue solid lines: by CSRZ; magenta dashed lines: 1D model; black solid lines: steady-state parallel plates model; yellow dashed lines: steady-state free space model; gray dashed lines: Gaussian bunch profile.

tions of wakefields in the vicinity of bunch center. Meanwhile, the discrepancy of amplitudes in the same area between CSRZ and steady-state models is attributed to entrance transient. Chamber shielding slightly suppresses the CSR wakefields at the bunch head part but enhances the wakefields at the bunch tail part. That is, the particles at the bunch tail part gain energy due to chamber shielding. Only when the bunch length is short enough, i.e. much less than $1/k_{th}$, chamber shielding is negligible.

The effect of CSR in the drift chamber after the exit of the bend is illustrated in Figs. 4-6. As observed from Fig. 4, with drift CSR neglected, the average slope of the imaginary part of CSR impedance is close to the free-space model at high frequency. But the average slope of the real part is slightly lower than the free-space model. This is due to the transient effect at the entrance part. The drift CSR changes the slope of both real and imaginary parts of CSR

impedance under the existence of straight chamber. This feature reveals the complexity of evaluating its effects on beam dynamics. The wake potentials corresponding to the impedances of Fig. 4 are shown in Fig. 5. One can easily see that the drift CSR causes additional energy loss and gain for particles in the vicinity of bunch centroid and in the bunch tail part, respectively.

Finally, we compare CSRZ results with the free-space model for drift CSR given in Ref. [13]. The results are shown in Fig. 6. It is seen that for bunch lengths longer than 1 ps, the free-space model overestimates the energy kick at the bunch centroid, and particles at the tail part gain energy due to chamber shielding.

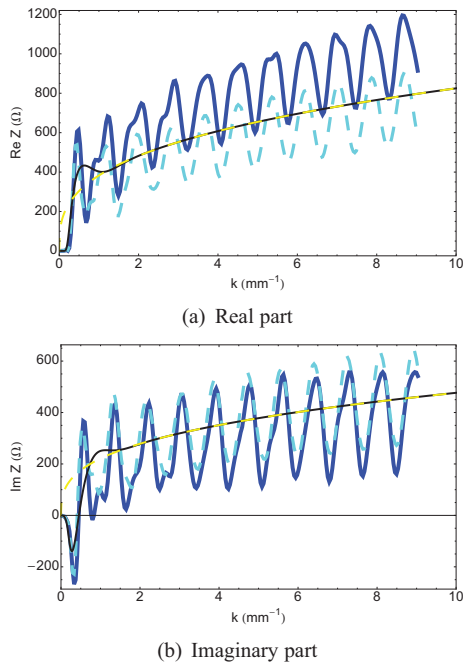


Figure 4: CSR impedance for a single bend in the cERL return loop with $\gamma = \infty$. Blue solid lines: with drift CSR considered; cyan dashed lines: with drift CSR neglected; black solid lines: steady-state parallel plates model; yellow dashed lines: steady-state free space model.

DISCUSSIONS AND TENTATIVE CONCLUSIONS

In this paper, the CSRZ code was used to investigate the properties of CSR impedance of a single bending magnet in the cERL return loop. It was found that chamber shielding causes remarkable energy kick, which is comparable to that felt by the particles at the bunch head part, to the particles at the bunch tail part in the cases of $\sigma_t > 2$ ps. When using the criterion of $\sigma_z \ll 1/k_{th}$ to estimate the shielding effect of vacuum chamber, it is suggested that the bunch length $\sigma_z = c\sigma_t$ should be replaced by the full bunch length, instead of the rms bunch length. Drift CSR wake is more sensitive to chamber shielding. The free-space model for drift CSR over-estimates the energy kick in the case of $\sigma_t > 1$ ps. Under bunch compression mode, the bunch will be compressed to rms length of 0.1 ps, and chamber shielding is fairly negligible. One minor point is that normal space-charge effects can be comparable to CSR effect at beam energy of $E = 35$ MeV or lower. More careful studies using macro-particle tracking simulations are underway to evaluate the space-charge effects and chamber shielding effects in CSR on beam dynamics.

The author would like to thank N. Nakamura for his interests in this work and M. Shimada and T. Miyajima for helpful discussions.

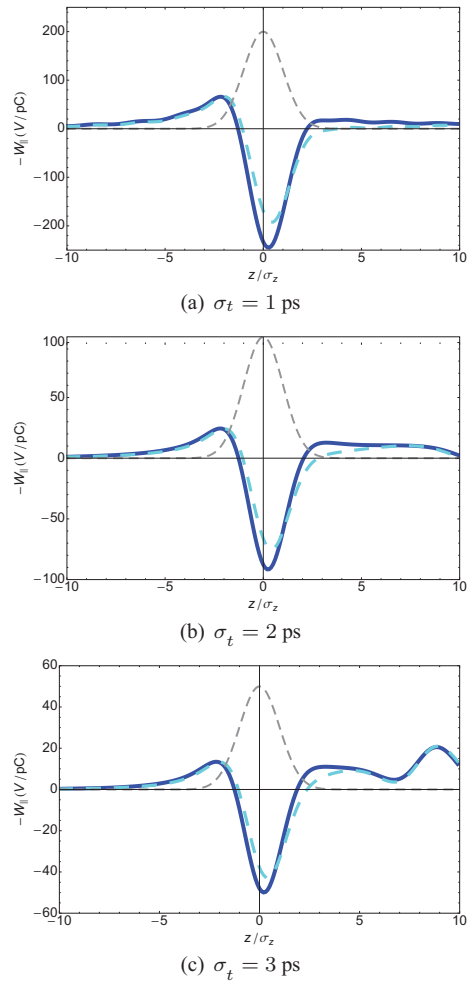


Figure 5: CSR wake potentials for a single bend in the cERL return loop with Gaussian bunch lengths of $\sigma_t = 1, 2, 3$ ps and $\gamma = \infty$. Blue solidlines: with drift CSR considered; cyan dashed lines: with drift CSR neglected; gray dashed lines: Gaussian bunch profile.

REFERENCES

- [1] T. Agoh and K. Yokoya, Phys. Rev. ST Accel. Beams, 7(5):054403 (2004).
- [2] D. Zhou, et al., IPAC'11, p.2268.
- [3] D. Zhou, et al., IPAC'11, p.604.
- [4] G. Stupakov and D. Zhou, SLAC-PUB-14332, December 9, 2010.
- [5] D. Zhou, PhD thesis, KEK/SOKENDAI, Sep. 2011.
- [6] M. Shimada, et al., IPAC'11, p.1909.
- [7] T. Agoh, Ph.D. thesis, University of Tokyo, 2004.
- [8] G. V. Stupakov and I. A. Kotelnikov, Phys. Rev. ST Accel. Beams, 12(10):104401 (2009).
- [9] A. Faltens and L. J. Laslett, Part. Accel. 4, 151. (1973).
- [10] T. Agoh, Phys. Rev. ST Accel. Beams, 12(9):094402 (2009).
- [11] M. Borland, Argonne National Laboratory Advanced Photon Source Report No. LS-287, 2000.
- [12] E. L. Saldin, et al., Nucl. Instrum. Methods Phys. Res., Sect. A, 398, 373 (1997).
- [13] G. Stupakov and P. Emma, LCLS-TN-01-12, December, 2001.

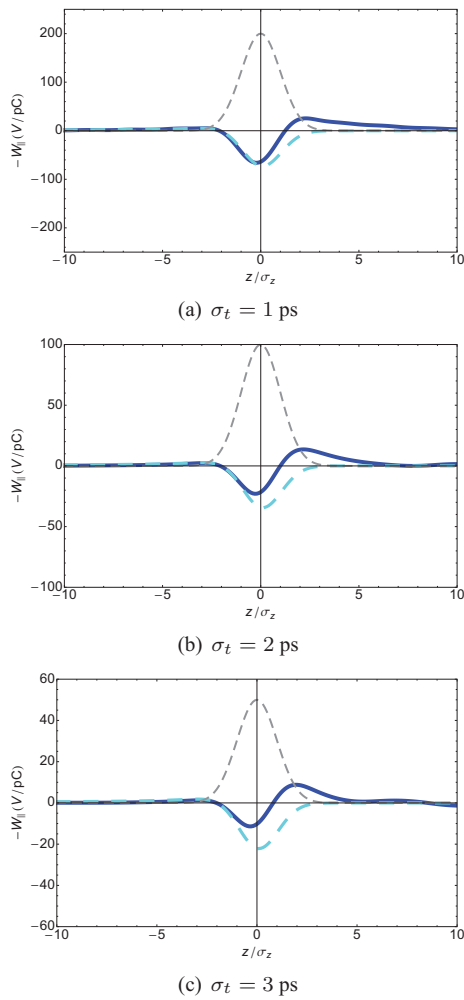


Figure 6: CSR wake potentials for a single bend in the cERL return loop with Gaussian bunch lengths of $\sigma_t = 1, 2, 3$ ps and $\gamma = \infty$. Blue solidlines: drift CSR by CSRZ; cyan dashed lines: drift CSR by Stupakov and Emma's free-space model; gray dashed lines: Gaussian bunch profile.